arXiv:astro-ph/0609736v1 27 Sep 2006

Draft: February 5, 2008

Improved $u'g'r'i'z'$ to $UBVR_CI_C$ Transformation Equations for Main Sequence Stars

Christopher T. Rodgers[1], Ron Canterna[1], J. Allyn Smith[1,2], Michael J. Pierce[1], and Douglas L. Tucker[3]

ABSTRACT

We report improved transformation equations between the $u'g'r'i'z'$ and $UBVR_CI_C$ photometric systems. Although the details of the transformations depend on luminosity class, we find a typical rms scatter on the order of 0.001 magnitude if the sample is limited to main sequence stars. Furthermore, we find an accurate transformation requires complex, multi-color dependencies for the bluer bandpasses. Results for giant stars will be reported in a subsequent paper.

Subject headings: Methods: data analysis — Standards: stars — techniques: photometric

1. Introduction

Stellar photometry has a long and successful history in the study of stellar properties. However, high precision photometry is necessary in order to enable accurate measurements of extinction, metallicity, and tests of stellar evolutionary models. Several filter systems have been developed over the last few decades with strengths and weaknesses associated with each (see (Straižys 1999) for a review). Recently, the Sloan Digital Sky Survey (hereafter SDSS; (York et al. 2000)) has greatly enhanced the available photometric data for Galactic stars and thereby promises to significantly add to our understanding of the Galaxy's stellar populations and formation history.

[1]University of Wyoming, Department of Physics & Astronomy, Laramie, WY 82071

[2]Los Alamos National Laboratory, ISR-4, D448, Los Alamos, NM 87545

[3]Fermi National Accelerator Laboratory, P.O. Box 500, Batavia, IL 60510

Although the $u'g'r'i'z'$ filter system was defined by Fukugita et al. (1996, F96) for the study of large scale structure and quasars in the northern galactic cap, these data have also provided a wealth of photometric data for Galactic stars (e.g. Newberg et al. 1999). Given the great potential of the SDSS data, we have begun a photometric study of star clusters in the $u'g'r'i'z'$ filter system (Rider et al. 2004; Moore et al. 2006; Smith et al. 2004). However, most of the existing photometric data and stellar evolutionary models are limited to the Johnson- Cousins $UBVR_CI_C$ filter system. Thus accurate transformation equations are necessary in order to evaluate the utility of the $u'g'r'i'z'$ filter system.

As part of the development of the SDSS photometric system, F96 derived preliminary transformation equations between the $UBVR_CI_C$ and $u'g'r'i'z'$ filters. These transformations were derived from the expected bandpasses, the predicted response of the SDSS detectors, and the spectral energy distribution of a metal poor, F subdwarf, specifically BD+17°4708. This star was chosen as the primary standard due to the availability of high precision, absolute spectrophotometry (see F96). The initial transformation equations of F96 were primarly intended to enable the simulation of the colors of various celestial objects. As a result, F96 assumed that the color transformation equations (e.g. $u' - g'$ vs. $U-B$) would be linear between the two photometric systems.

More accurate empirical transformations were derived by Smith et al. (2002) from $u'g'r'i'z'$ photometry of a subset of the $UBVR_CI_C$ standard stars from Landolt (1992). Smith et al. (2002) also assumed a linear transformation and made no distinction between luminosity classes among their standard stars. Finally, more complex transformations for UBV to $u'g'r'$ filters were presented by Karaali et al. (2005). These equations include two Johnson colors for the $u' - g'$ and $g' - r'$ relations, but do not make a distinction between luminosity classes. In this paper we re-examine Smith et al. (2002) data with the goal of deriving more accurate transformation equations between these two photometric systems. In §2 we describe our analysis procedure and §3 contains our results. In §4 we present our conclusions and describe our ongoing efforts to expand the analysis to other luminosity classes.

2. Transformation Equations Between the $u'g'r'i'z'$ and $UBVR_CI_C$ Systems

2.1. Astrophysical Issues

The data (Table 1) used for this analysis is drawn from the available photometry of the equatorial region standard stars in common between the $UBVR_CI_C$ (Landolt 1992) and the $u'g'i'r'z'$ filter systems (Smith et al. 2002). Figure 1 show these data along with the color-color

relations for stars of various luminosity classes (Johnson et al. 1966). The latter were slightly smoothed and transformed onto the Cousins system (Cousins 1976) using the transformations derived by Fernie (1983). Figure 1 illustrates the dependence of the transformations upon luminosity class. Due to the limited number of known luminosity class stars, we assumed that stars with unknown luminosity class that lie along the ZAMS are of luminosity class V. The stars with unknown luminosity class that lie in the regions of luminosity degeneracy (where the luminosity class relations cross each other) are still considered unknown. The star with one exception to all of these restrictions is Ru-152. This star is published as an O5V, but since it lies so close to the supergiant relation, it must either be evolved or it is highly reddened. In any case, this star must be considered unknown as well. Since the number of available supergiants and giants is limited, this paper will only address the transformation for main sequence (luminosity class V) stars.

Inspection of the normalized response filter curves shown in Figure 2 suggests that the system transformation relations should be a function of two colors for most of the filter combinations. That is, the u' filter is closely related to the U filter, but the g' filter bandpass spans both B and V filters. Thus, the $u' - g'$ color should be dependent on not only the $U - B$ color, but also the $B - V$ color. Likewise, because the V filter samples portions of both g' and r' filters, the $g' - r'$ color should depend on both the $B - V$ and $V - R_C$ colors. The situation for the i' and z' filters and associated colors is less clear since the z' bandpass does not lie within the Johnson system and is a function of the detector being used and will vary from instrument to instrument.

It is also evident from Figure 2 colors involving the redder bandpasses of both filter systems will be affected by the TiO molecular bands present in later spectral types (cooler stars). Unfortunately, there is a deficiency in the available data for stars of later spectral type (see Figure 1). Therefore, our analysis will be further restricted to stars with $B - V < 1.3$ (see Table 1).

2.2. Analysis Procedure

The transformation equations for each color were obtained using the `IDL REGRESS` (two dimensional, multi-variable fitting) and `POLY_FIT` (two dimensional fitting) programs. Each $u'g'r'i'z'$ color was fit using both single and multi-color combinations of Johnson colors. Although higher order fits were examined, the first order fits were found to be suffecient. The chi-square is examined for each fit and the relative error in each coefficient in order to minimize the statistical errors. Finally, we did a "by eye" inspection of the fits to verify that the results made physical sense.

3. Results

We now address our results for each $u'g'r'i'z'$ color combination individually.

3.1. The $u' - g'$ Equation

The $u' - g'$ color is very complex in terms of the UBV filters. The Balmer discontinuity for MS stars affect the color in $U - B$. When the opacity source changes at A0 type stars, the $U - B$ color makes a dramatic change in color. This effect also occurs in $u' - g'$ since the filters span the Balmer Jump as well. Moreover, the g' filter is sensitive to temperature changes in the star. $B - V$ is also sensitive to temperature, so the $u' - g'$ color is temperature dependent. With these two factors in mind, we used a first order mulit-variable polynomial as the basis for this first transformation equation.

Since we are using main sequence (MS) stars, we will use the Morgan & Keenan ZAMS (Johnson et al. 1966) in all subsequent figures to show the validity of each transformation by color. Our transformation equation for the MS stars in $u' - g'$ is:

$$u' - g' \;=\; 1.101(\pm 0.004)(U - B) + 0.358(\pm 0.004)(B - V) + 0.971 \; . \qquad (1)$$

Figures 3 and 4 shows the ZAMS fit in the both the $u' - g'$ vs. $U - B$ and $u' - g'$ vs. $B - V$ color-color planes with residuals for comparison of Karaali et al. (2005). As an illustration that our new fit is more accurate, we have properly fit the Balmer discontinuity. The $u' - g'$ vs. $B - V$ plane resembles a standard color-color diagram with the data nicley fitting the ZAMS when the residuals are compared. The chi-square to each final color fit are givin in Table 2.

3.2. The $g' - r'$ Equation

The r' filter maps most directly to the R filter while the g' filter overlaps both the B and V filters. Therefore, we would expect a strong dependance of $g' - r'$ on both $B - V$ and $V - R_C$. But before fitting this data set, the physical properties of extremely red stars must be taken into account. In stars with $V - R_C > 0.8$, molecular TiO bands start to dominate the stellar profile. Since our data set contains only three stars this red an accurate transformation determination cannot be obtained after $V - R_C = 0.8$. Therefore, these three data points have been dropped from the final $g' - r'$ fit.

Figure 5 shows the ZAMS fit of $g' - r'$ vs. $B - V$ and $g' - r'$ vs. $V - R_C$ with the residuals of Karaali et al. (2005) and this paper. Notice that Karaali et al. (2005) residuals in the $g' - r'$ vs. $V - R_C$ color-color plane are not available because Karaali et al. (2005) did not use the $V - R_C$ color in their transformation equations. The $g' - r'$ relation now becomes:

$$g' - r' = 0.278(\pm 0.016)(B - V) + 1.321(\pm 0.030)(V - R_C) - 0.219 \ . \quad (2)$$

3.3. The $r' - i'$ and $r' - z'$ Equations

Both the $r' - i'$ and $r' - z'$ relations are relatively simple compared to the previous two equations since the r' and R_C filters have roughly the same effective wavelength and bandpass, and the I_C filter is mapped only by the i' and z' filters. For this reason, both of the SDSS colors will be dependent upon $R_C - I_C$ only. We performed a least squares polynomial fit to the data using the same in the $g' - r'$ data due to the lack of data for TiO bands in M stars. Figure 6 and Figure 7 show the $r' - i'$ vs. $R_C - I_C$ and $r' - z'$ vs. $R_C - I_C$ final fits with their respective residuals. Notice that the data follow a well defined linear relation. The equations for $r' - i'$ and $r' - z'$ are simply:

$$r' - i' = 1.000(\pm 0.006)(R_C - I_C) - 0.212 \ , \quad (3)$$
$$r' - z' = 1.567(\pm 0.020)(R_C - I_C) - 0.365 \ . \quad (4)$$

3.4. The $g' - V$ Equation

The $g' - V$ color relation is derived mostly for convience to the user. In order to obtain individual magnitudes in each of the $u'g'r'i'z'$ filters, we need a logical color-color relation that will give the user the ability to obtain one of the filter magnitudes. Since the Johnson V is often cited as the base magnitude for most published values, the g' filter is the most logical choice to obtain V magnitudes. Since the g' filter bandpass covers the B and V filter bandpasses, the relation will be derived using a $B-V$color. We did a least squares polynomial fit to the data using all the available data in Table 1 excluding Ru-152. Figure 8 illustrates the results of this fit with the residuals. The equation for this relation is:

$$g' - V \;=\; -0.042(\pm 0.007)(B-V)^2 + 0.602(\pm 0.011)(B-V) - 0.087\ . \qquad (5)$$

4. Conclusions

Comparing the residuals and the actual plots for each color transformation demonstrates that our new transformation equations give better results for MS stars than Karaali et al. (2005) and Smith et al. (2002). Additional work remain to fully develop the complete set of transformation equations for all luminosity classes. First, more data is needed for extremely red MS stars ($B - V > 1.3$). Also, an investigation of the effects of metallicity on the transformations for each class of star must be undertaken. This means that other isochrone models of $u'g'r'i'z'$ interest, with existing $UBVR_CI_C$ data (such as Y^2; (Yi et al. 2001)), must be identified and transformed. This is a complicated and time consuming prospect, but with the advent of high-precision photometry, it must be completed in order to deliver the accuracies needed when describing stellar systems.

We plan to pursue this endeavor in future work. A beginning step is the development of a full metallicity and luminosity photometric study in the $u'g'r'i'z'$ filter system. This study has all ready begun using the 0.6m telescope at Red Buttes Observatory in Laramie, Wyoming to support the extension of the Sloan Digital Sky Survey.

CTR, JAS, and DLT acknowledge support from National Science Foundation Grant No. 0098401. JAS acknowledges support from the Los Alamos National Laboratory LDRD program 20030486DR. RC, CTR, and MJP acknowledge support from EPSCoR grant No. NCC5-578.

REFERENCES

Cousins, A. W. J. 1976 MRAS, 81 25

Fernie, J. D. 1983 PASP, 95, 782

Fukugita, M., Ichikawa, T., Gunn, J. E., Doi, M., Shimasaku, K., & Schneider, D. P. 1996, AJ, 111, 1748

Johnson, H. 1966 ARA&A, 4, 193

Karaali, S., Bilir, S., Tunçel, S. 2005, PASA, 22, 24

Landolt, A. U. 1992, AJ, 104, 336

Moore, D. C., Tucker, D. L., Smith, J. A., Stoughton, C., Rider, C. J., Allam, S. S., & Rodgers, C. T. 2006, AJ, submitted

Newberg, H. J., Richards, G. T., Richmond, M., & Fan, X. 1999, ApJS, 123, 377

Rider, C. J., Tucker, D. L., Smith, J. A., Stoughton, C., Allam, S. S., & Neilsen, E. H. 2004, AJ, 127, 2210

Smith, J. A. et al. 2004, BAAS, 205, 6409

Smith, J. A., Tucker, D. L., Kent, S. et al. 2002, AJ, 123, 2121

Stoughton, C., Lupton, R. H., Bernardi, M. et al. 2002, AJ, 123, 485

Straižys 1999, BaltA, 8, 505

Yi, S., Demarque, P., Kim, Y., Lee, Y., Ree, C. H., Lejeune, T., & Barnes, S. 2001, ApJS, 136, 417

York, D. G., Adelman, J., Anderson, J. E. et al. 2000, AJ, 120, 1579

This preprint was prepared with the AAS LaTeX macros v5.2.

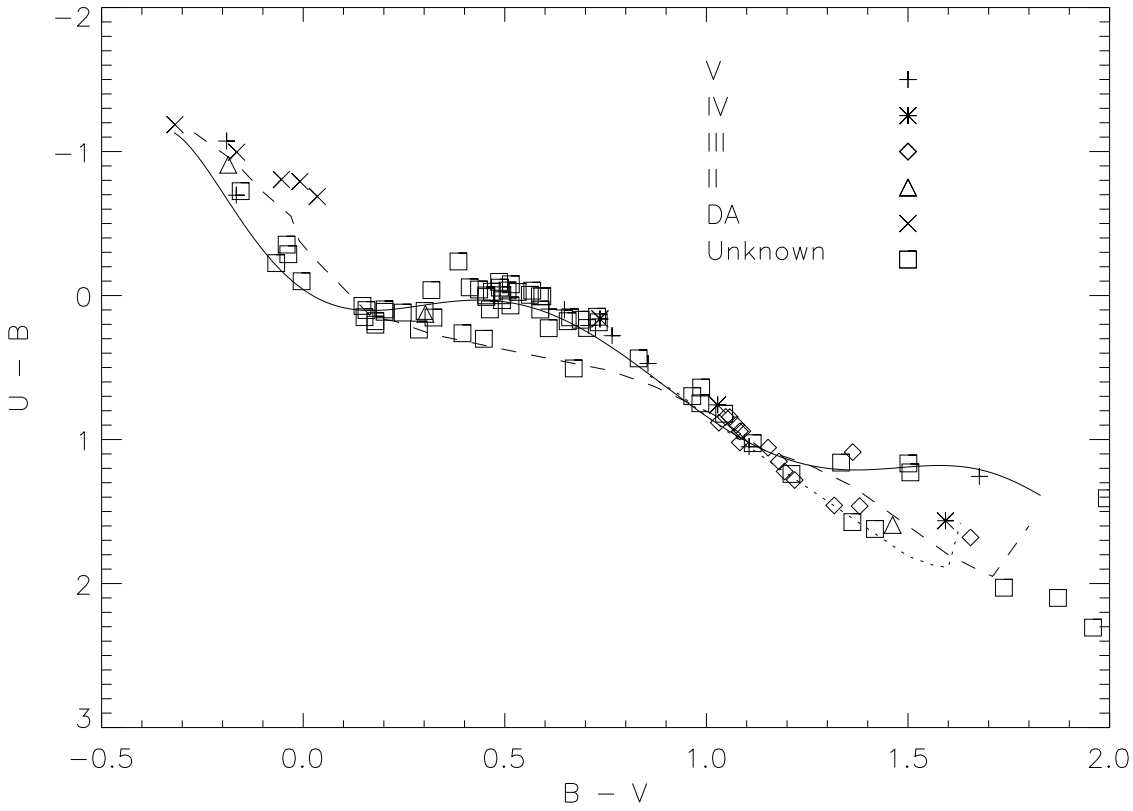

Fig. 1.— A UBV color-color diagram of the data set used in the Smith et al. (2002) transformation equations. The solid line is the smoothed ZAMS relation (luminosity class V), the dotted line is the giants relation (luminosity class III), and the dashed line is the supergiants relation (luminosity class I) taken from Johnson et al. (1966). The different symbols give the corresponding known and unknown luminosity classes for the stars from Smith et al. (2002). Using the luminosity class V stars and well placed but unknown spectral class stars which lie along the ZAMS, we will create new transformation equations that satisfy these data. Note that Ru-152 (-0.190, -1.073) will not be included due to high reddening.

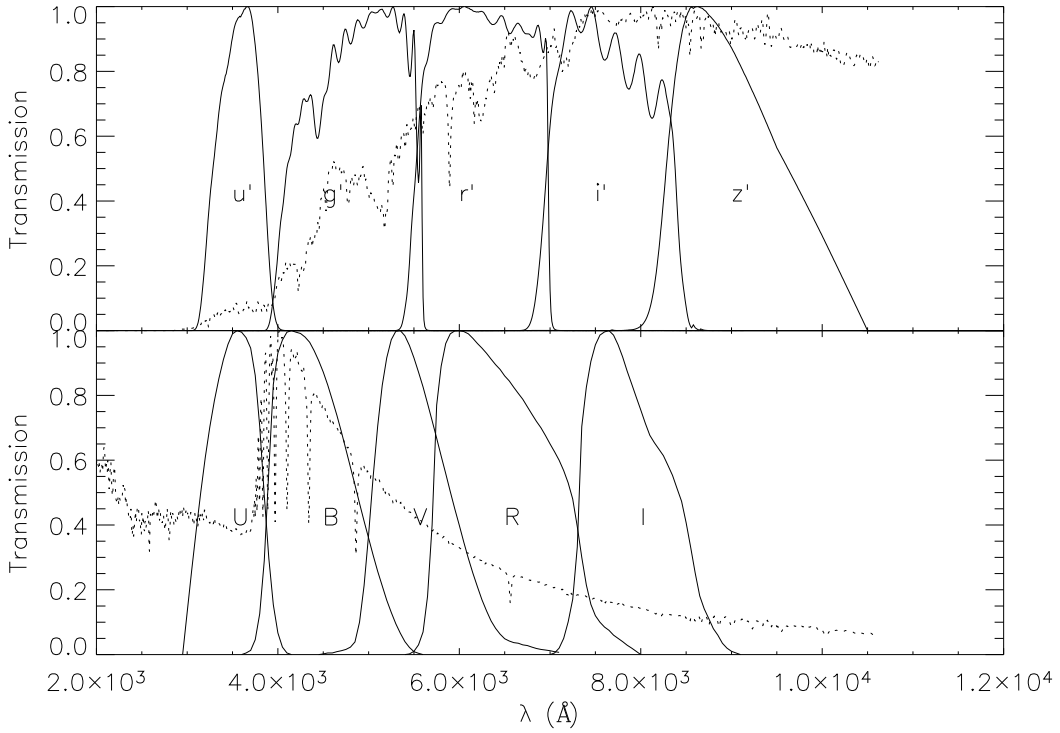

Fig. 2.— The normalized transmission curves for $UBVR_CI_C$ and $u'g'r'i'z'$ filter systems. Overplotted in the upper and lower panels is a M0 V and A0 V spectral energy distributions. Some problems that will arise from the physical aspects of these stars occur from first the Balmer discontinuity, second the TiO bands in latter type stars (i.e. M0 V), and third the change of the main opacity source at $T_eff = 10,000K$. The Balmer discontinuity will effect the $u' - g'$ and $U - B$ colors. The TiO bands will effect $r' - i'$, $r' - z'$, $V - R_C$, and $R_C - I_C$ colors. The change in opacity source at $T_eff = 10,000K$ will effect the $u' - g'$, $U - B$, and $g' - r'$ colors.

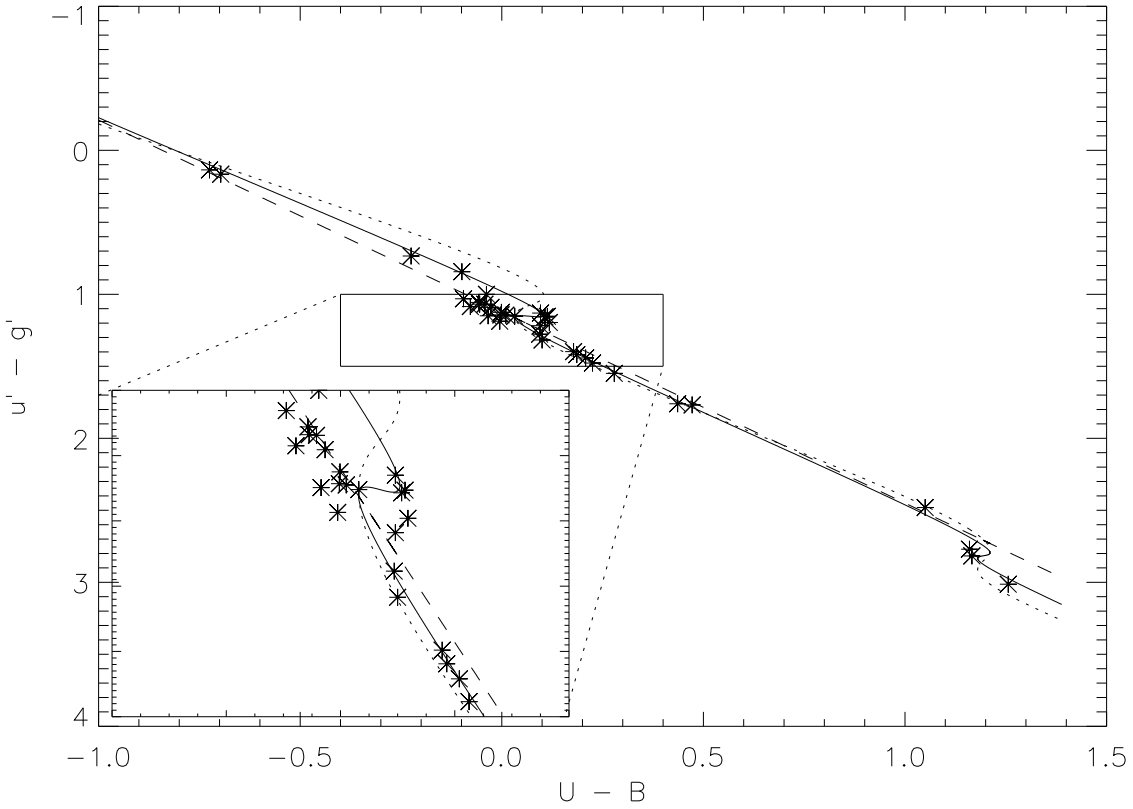

Fig. 3.— The $u' - g'$ transformation equation fit shown here with a two dimensional cut of $u' - g'$ vs. $U-B$. Figure 4 gives the $u' - g'$ vs. $B-V$ two dimensional cut. The solid line is this paper's fit, the dotted line is the Karaali et al. (2005) fit, and the dashed line is the Smith et al. (2002) fit for the $u' - g'$ fit. The inset is an expanded view of the Balmer Jump region located in the boxed region. Notice in the zoomed in section that the Balmer discontinuity region of the $u'-g'$ vs. $U-B$ has been accurately fit by the new transformation equation.

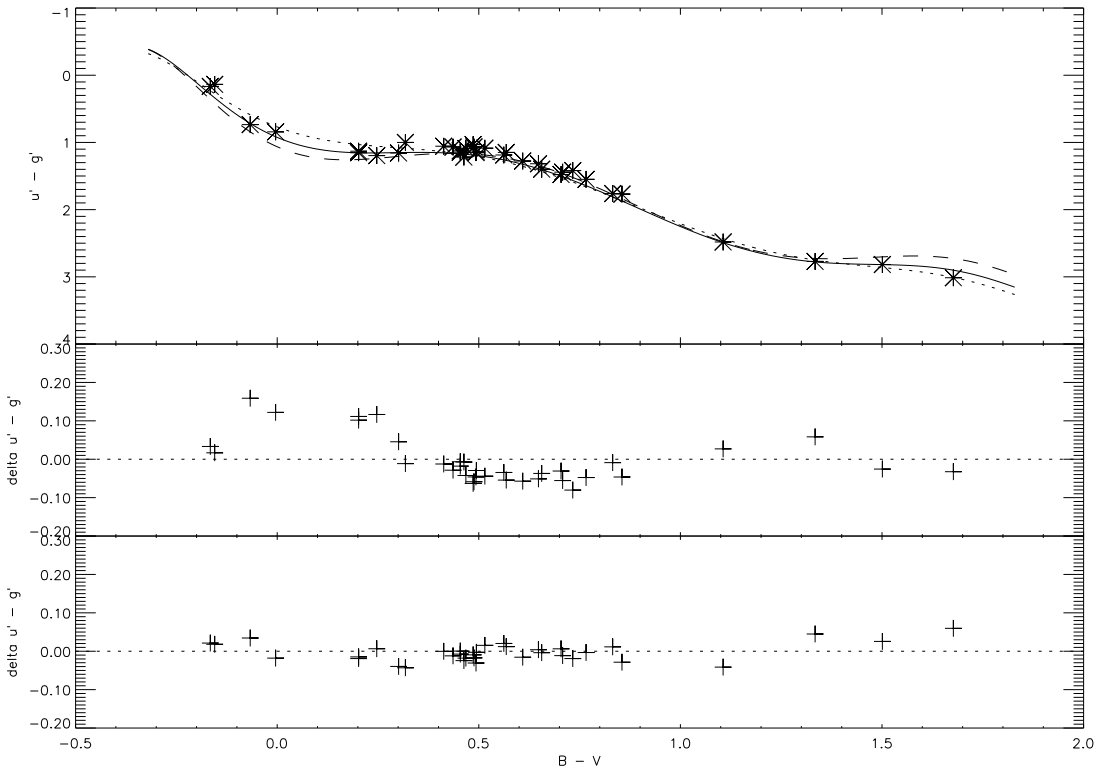

Fig. 4.— The $u' - g'$ transformation equation fit shown here with a two dimensional cut of $u' - g'$ vs. $B-V$. The lines seen in the top panel are the same as in Figure 3. The bottom panel gives the residuals for both the Karaali et al. (2005) fit (middle) and this paper's fit (bottom).

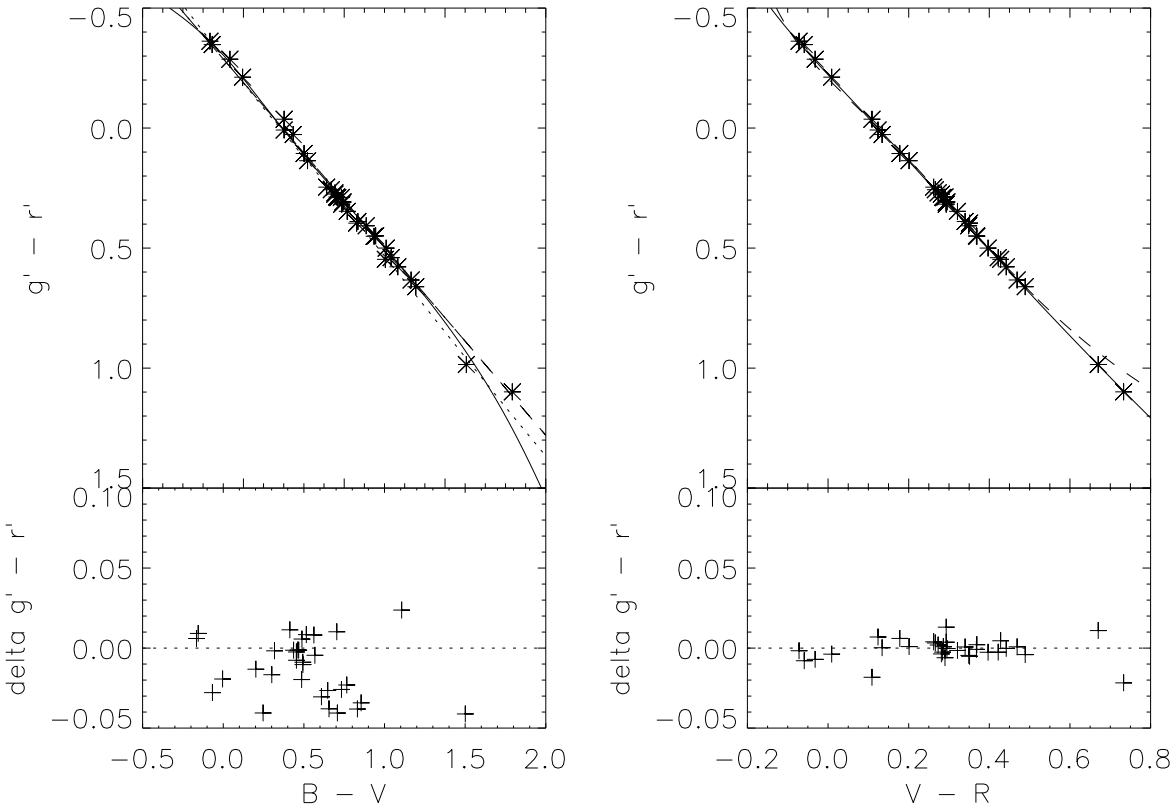

Fig. 5.— The $g' - r'$ transformation equation fit shown here with a two dimensional cut of $g' - r'$ vs. $B-V$ (left) and $V - R_C$ (right without Karaali et al. (2005) fit since there is no $V - R_C$ dependence in their fits). The lines in the top panels are the same as in Figure 3. The bottom panels give the residuals for this paper's (right) and Karaali et al. (2005) (left).

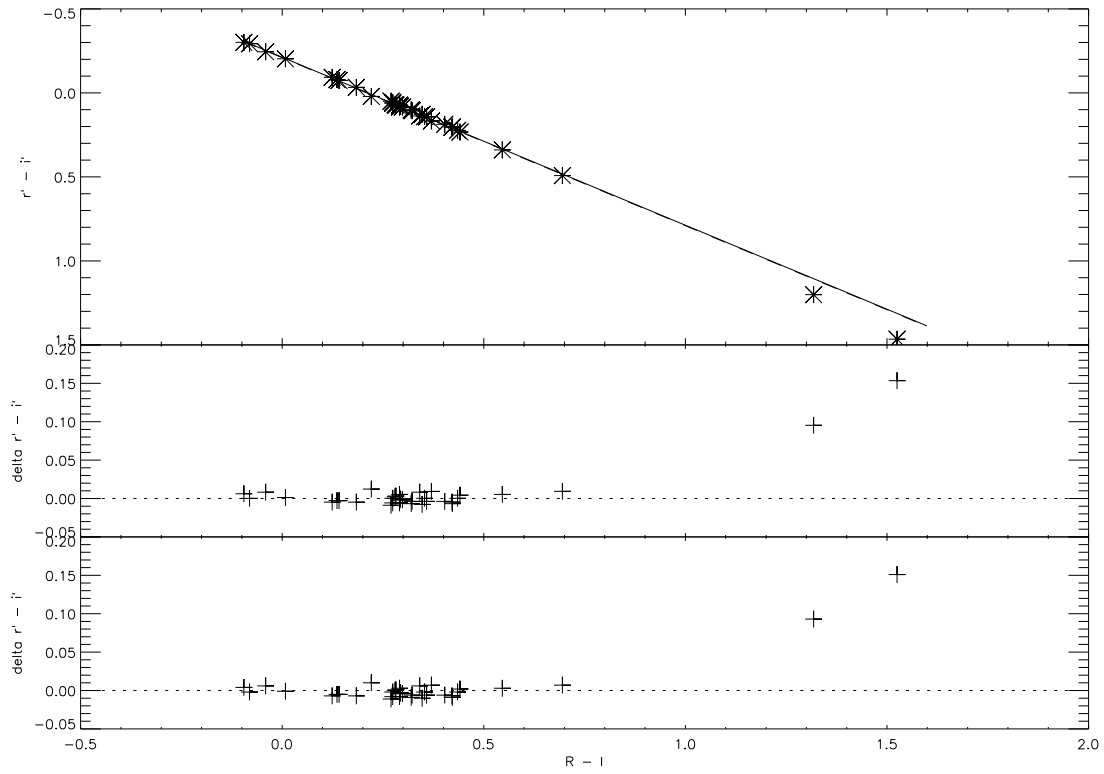

Fig. 6.— The $r' - i'$ transformation equation fit with residuals using the Smith et al. (2002) fit (middle) and this paper's fit (bottom). The lines in the top panels are the same as in Figure 3. The two extreme red points were not included within the fit due to insufficient data for stars with $B - V > 1.3$.

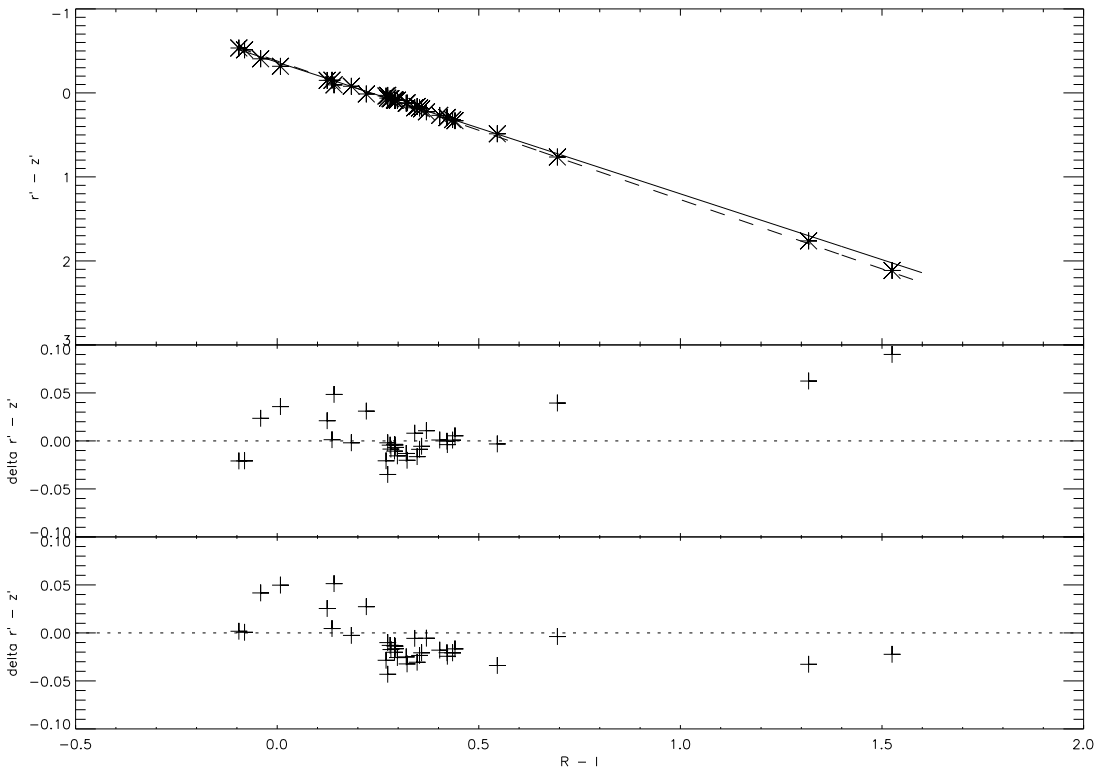

Fig. 7.— The $r' - z'$ transformation equation fit with residuals using the Smith et al. (2002) fit (middle) and this paper's fit (bottom). The lines in the top panels are the same as in Figure 3. The two extreme red points were not included within the fit due to insufficient data for stars with $B - V > 1.3$.

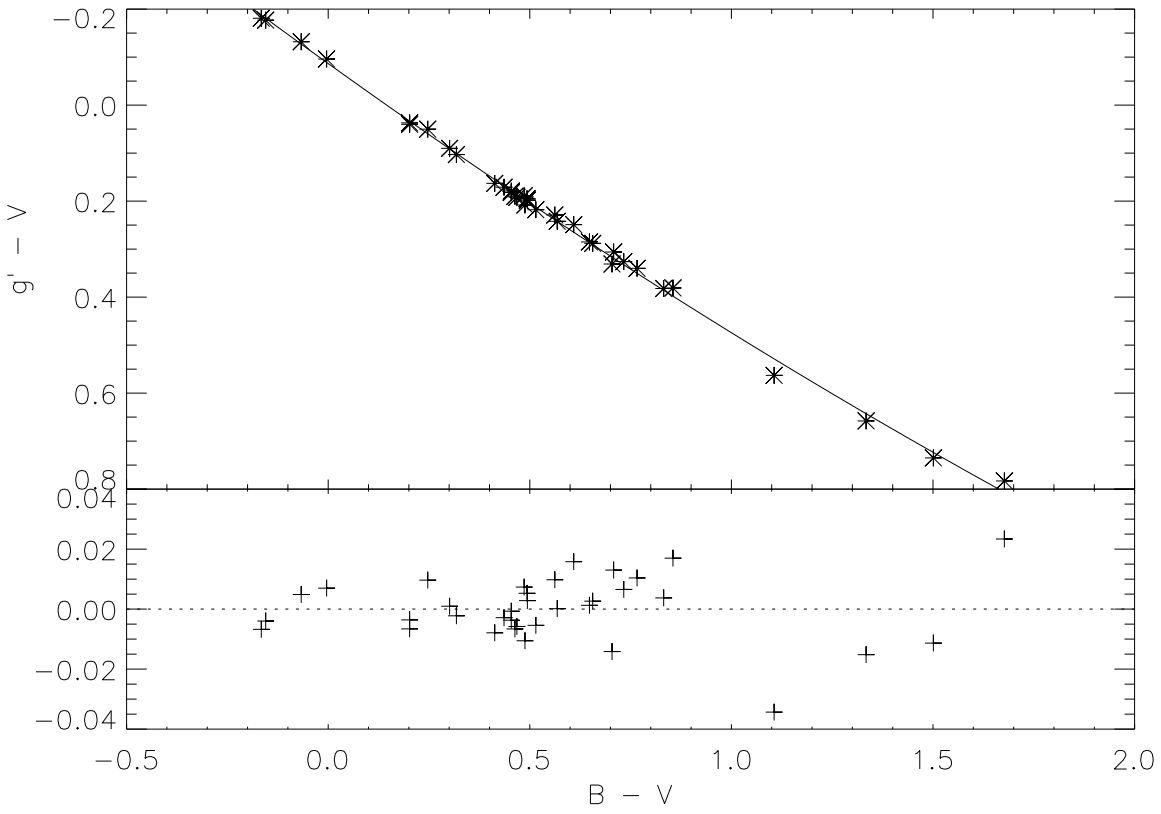

Fig. 8.— The $g' - V$ transformation equation fit with residuals from this paper's fit. This was created for convenience of the user to acquire individual magnitudes in the $u'g'r'i'z'$ filter system.

Table 1. Standard Star Data Set

Name	V	$B-V$	$U-B$	$V-R$	$R-I$	$u'-g'$	$g'-r'$	$r'-i'$	$i'-z'$
92-342	11.613	0.436	-0.042	0.266	0.270	1.069	0.257	0.049	-0.012
92-502	11.812	0.486	-0.095	0.284	0.292	1.031	0.289	0.078	0.010
92-282	12.969	0.318	-0.038	0.201	0.221	1.000	0.136	0.021	-0.009
92-288	11.630	0.855	0.472	0.489	0.441	1.768	0.661	0.233	0.098
93-317	11.546	0.488	-0.055	0.293	0.298	1.068	0.317	0.084	0.002
93-333	12.011	0.832	0.436	0.469	0.422	1.760	0.633	0.203	0.089
94-242	11.728	0.301	0.107	0.178	0.184	1.157	0.106	-0.033	-0.046
95-96	10.010	0.147	0.072	0.079	0.095	1.142	-0.070	-0.123	-0.051
95-218	12.095	0.708	0.208	0.397	0.370	1.442	0.500	0.167	0.058
95-236	11.491	0.736	0.162	0.420	0.411	1.414	0.539	0.196	0.084
96-36	10.591	0.247	0.118	0.134	0.136	1.196	0.027	-0.079	-0.072
96-737	11.716	1.334	1.160	0.733	0.695	2.770	1.099	0.492	0.271
96-83	11.719	0.179	0.202	0.093	0.097	1.237	-0.054	-0.110	-0.048
97-249	11.733	0.648	0.100	0.369	0.353	1.317	0.451	0.141	0.038
97-351	9.781	0.202	0.096	0.124	0.141	1.130	0.008	-0.074	-0.022
98-978	10.572	0.609	0.094	0.349	0.322	1.277	0.407	0.106	0.013
98-185	10.536	0.202	0.113	0.109	0.124	1.153	-0.037	-0.093	-0.057
98-653	9.539	-0.004	-0.099	0.009	0.008	0.843	-0.212	-0.203	-0.114
98-685	11.954	0.463	0.096	0.290	0.280	1.218	0.287	0.070	-0.001
Ru-152	13.014	-0.190	-1.073	-0.057	-0.087	-0.263	-0.355	-0.289	-0.252
99-438	9.398	-0.155	-0.725	-0.059	-0.081	0.136	-0.348	-0.293	-0.220
99-447	9.417	-0.067	-0.225	-0.032	-0.041	0.734	-0.287	-0.245	-0.161
100-241	10.139	0.157	0.101	0.078	0.085	1.165	-0.068	-0.128	-0.097
100-280	11.799	0.494	-0.002	0.295	0.291	1.143	0.308	0.084	0.003
BD-12:2918	10.067	1.501	1.166	1.067	1.318	2.817	1.326	1.201	0.561
101-316	11.552	0.493	0.032	0.293	0.291	1.152	0.309	0.073	0.007
101-207	12.419	0.515	-0.078	0.321	0.320	1.085	0.347	0.101	0.022
103-626	11.836	0.413	-0.057	0.262	0.274	1.056	0.246	0.056	-0.027
104-598	11.479	1.106	1.050	0.670	0.546	2.481	0.985	0.339	0.148
DM+2_2711	10.367	-0.166	-0.697	-0.072	-0.095	0.166	-0.362	-0.301	-0.234
107-1006	11.712	0.766	0.279	0.442	0.421	1.549	0.578	0.204	0.090
107-351	12.342	0.562	-0.005	0.351	0.358	1.187	0.396	0.142	0.048
108-551	10.703	0.179	0.178	0.099	0.110	1.256	-0.032	-0.104	-0.051
Wolf629	11.759	1.677	1.256	1.185	1.525	3.013	1.413	1.466	0.648
109-381	11.730	0.704	0.225	0.428	0.435	1.477	0.547	0.223	0.094
112-223	11.424	0.454	0.010	0.273	0.274	1.145	0.270	0.062	0.000
112-805	12.086	0.152	0.150	0.063	0.075	1.183	-0.087	-0.135	-0.090

Table 1—Continued

Name	V	$B-V$	$U-B$	$V-R$	$R-I$	$u'-g'$	$g'-r'$	$r'-i'$	$i'-z'$
113-339	12.250	0.568	-0.034	0.340	0.347	1.149	0.389	0.127	0.035
113-466	10.004	0.454	-0.001	0.281	0.282	1.125	0.275	0.073	-0.005
114-531	12.094	0.733	0.186	0.422	0.403	1.419	0.540	0.187	0.080
114-654	11.833	0.656	0.178	0.368	0.341	1.398	0.449	0.137	0.040
114-750	11.916	-0.041	-0.354	0.027	-0.015	0.548	-0.212	-0.230	-0.163
115-420	11.161	0.468	-0.027	0.286	0.293	1.091	0.290	0.080	0.007
115-516	10.434	1.028	0.759	0.563	0.534	2.167	0.807	0.317	0.172

Table 2. Reduced χ^2

Color	Reduced χ^2
$u' - g'$	0.0003
$g' - r'$	0.001
$r' - i'$	0.001
$r' - z'$	0.011